ARTICLE

Crystal Structure, Fe^{3+} Luminescence Sensing and Color Tuning of 2*D* Lanthanide-metal-organic Frameworks Constructed from Tricarboxylic Acid Ligand①

PAN Meng-Qi[a] YANG Run-Qi[a] MUHAMMAD Yaseen[b]
CAI Kun-Tong[a] HAN Feng[a] ZHANG Hao-Chen[a]
NIU Yuan-Qing[a] WANG Hao[a]②

[a] (*Beijing Key Lab of Special Elastomer Composite Materials, College of New Materials and Chemical Engineering, Beijing Institute of Petrochemical Technology, Beijing* 102617, *China*)

[b] (*Institute of Chemical Sciences, University of Peshawar, Peshawar* 25120, *Pakistan*)

ABSTRACT A new lanthanide metal-organic framework (MOF) [Eu(BTB)(phen)(DMF)]·DMF (**1**, DMF = N,N-dimethylformamide) was synthesized using H_3BTB (1,3,5-tri(4-carboxyphenyl)benzene) and phen (1,10-phenanthroline) under solvothermal conditions. The structure of the prepared MOF was characterized by single-crystal X-ray diffraction analyses, elemental analysis, fluorescence spectrum, FT-IR spectroscopy, powder X-ray diffraction and thermogravimetric analyses. The structure of **1** can be viewed as a 3-*D* supramolecular network, which is formed by the stacking of 2*D* layers through *π*-*π* interaction. The luminescence explorations revealed that **1** possesses favorable selectivity and sensitivity for testing Fe^{3+}. Additionally, color tuning was achieved by varying Eu^{3+}:Tb^{3+} ratios in the reaction mixtures.

Keywords: lanthanide metal-organic frameworks, sensing, luminescence, Fe^{3+}, color tuning;

DOI: 10.14102/j.cnki.0254-5861.2011-3243

1 INTRODUCTION

Iron(III), as an indispensable trace elements of our life, plays an important role in a number of physiological processes such as DNA synthesis, hemoglobin formation, oxygen transport and storage, and coordination of brain functions[1-5]. However, the presence of a large amount of iron(III) is harmful to humans[6, 7], causing damages to heart, liver, and other vital organs through the blood circulation, and hence in turn affects the absorption of other elements[8, 9]. Therefore, detection of iron(III) in human body is getting greater attention where luminescent sensing has been marked as an efficient tool to achieve this task based on simplified and convenient operation[10-12].

Recently, metal-organic frameworks (MOFs) as new materials have been widely applied in numerous areas, including gas storage and separation, catalysis, optoelectronics, energy storage and conversion, photocatalysis and luminescence and sensing[13-24]. As a promising subfamily of MOFs, lanthanide based MOFs (Ln-MOFs) have attracted great attention for their significant luminescent properties because of the intrinsic features of lanthanide elements. Ln-MOFs have unique advantages and properties due to the 4*f* electron configuration of the lanthanide metal, such as strong absorption and inherent luminescence band of lanthanides, large Stokes shift, pure color, and relatively long luminescence lifetime, which make them receive more attention in luminescence sensing[25-33]. Furthermore, the fluorescent properties of Ln-MOFs can be further modulated by both analyte-metal and analyte-ligand interactions since the unique luminescence mechanism involves ligand-to-metal energy transfer (LMET)[34-36]. In particular, Eu^{3+} and Tb^{3+} based complexes have great significance for the luminescent studies because they can emit strong characteristic red or green light when excited by energy transfer from the ligand to the lanthanide ion via UV radiation. Moreover, mixed-Ln-

Received 30 April 2021; accepted 15 July 2021 (**CCDC 2079858**)

① This project was supported by the High-level Teachers in Beijing Municipal Universities in the Period of 13th Five-year Plan (CIT&TCD201904044) and URT program of Beijing Institute of Petrochemical Technology (2020J00009)

② Corresponding author. Wang Hao, E-mail: wangh@bipt.edu.cn

MOFs can be obtained through integrating Eu^{3+} and Tb^{3+} into a single crystal of Ln-MOFs, which can effectively combine dual-luminescent centers to generate multicolored emission materials. In general, the changes in the emission color can be effectively modulated by changing the mixing ratios of Eu^{3+}:Tb^{3+}[37, 38].

In our previous study, we have reported that some Ln-MOFs show sensitive response to nitrobenzene through fluorescence quenching mechanism[39]. In continuation to that study, herein we report the synthesis of a new Eu-MOF (**1**) by a solvothermal method using 1,3,5-tri(4-carboxyphenyl)benzene (H_3BTB) as ligand for that polycarboxylic acids have rich coordination modes and strong coordination ability[40-43]. **1** is a two-dimensional (2*D*) laminar structure, and the three-dimensional (3*D*) structure was formed by the stacking of the 2*D* layers through π-π interactions. The luminescence explorations revealed that **1** possesses good selectivity and sensitivity for the sensing of Fe^{3+}. Additionally, color tuning in Eu^{3+}/Tb^{3+} systems was achieved by varying lanthanide ions ratios in the reaction mixture.

2 EXPERIMENTAL

2. 1 Materials and instruments

All the chemicals including H_3BTB used in this study were of analytical grade and commercially available.

The luminescence spectra and sensing properties for the powdered solid samples were measured on an Edinburgh FS5 spectrophotometer under identical experimental conditions. Fourier transform infrared (FTIR) spectra were obtained on a Tensor 27 OPUS (Bruker) FT-IR spectrometer in a wavenumber range of 400～4000 cm^{-1}. Thermogravimetric (TG) analysis was carried out on a Rigaku standard TG-DTA analyzer at a heating rate of 10 ℃·min^{-1} from ambient temperature to 800 ℃ using an empty Al_2O_3 crucible as a reference. The powder X-ray diffraction spectra (PXRD) were recorded on a Rigaku D/Max-2500 diffractometer at 40 kV, 100 mA for a Cu-target tube, and a graphite monochromator. Simulation of the PXRD pattern was carried out by the single-crystal data and diffraction-crystal module of the Mercury (Hg) program version 1.4.2. Elemental analyses (C, H and N) were performed on a Perkin-Elemer240C analyzer.

2. 2 Synthesis and crystallization

2. 2. 1 Synthesis of [Eu(BTB)(phen)(DMF)]žDMF (1)

1 was synthesized using solvothermal method. A mixture of $Eu(NO_3)_3·6H_2O$, H_3BTB, 1,10-phenanthroline, and 5 mL DMF:H_2O (*v*:*v* = 1:1) was added to a glass bottle, heated at 95 ℃ for 3 days, and then cooled to room temperature. The heterogeneous solution was separated from the solid phase and the crystals were washed with ethanol and dried at room temperature. Colorless block crystals were obtained. The net yield of various components was: 25%. Anal. Calcd. for $C_{45}H_{37}EuN_4O_8$ (%): C, 59.14; H, 4.05; N, 6.13. Found (%): C, 59.06; H, 4.15; N, 6.10. FT-IR (KBr pellets, cm^{-1}): 3444 w, 1650 m, 1582 s, 1520 s, 1409 s, 1182 w, 1104 w, 1014 w, 963 w, 859 w, 787 s, 730 w.

2. 2. 2 Synthesis of [Eu_xTb_{1-x}(BTB)(phen)(DMF)]žDMF (2～5)

Eu_xTb_{1-x}-MOF were synthesized according to a similar procedure to that of **1** except doping a certain amount of $Tb(NO_3)_3·6H_2O$ instead of $Eu(NO_3)_3·6H_2O$. The percentage of $Tb(NO_3)_3·6H_2O$ was 90.91% (**2**), 98.04% (**3**), 99.01% (**4**) and 100% (**5**), respectively. Complex **2**: yield: 23%. Anal. Calcd. for $C_{45}H_{37}Eu_{0.0909}Tb_{0.9091}N_4O_8$: C, 58.74%; H, 4.05%; N, 6.09%. Found: C, 58.82%; H, 4.12%; N, 6.15%. FT-IR (KBr pellets, cm^{-1}): 3440 m, 3444 w, 1650 m, 1606 w, 1581 m, 1531 s, 1411 s, 1182 w, 1105 w, 1014 w, 860 m, 786 s, 730 m, 667 w, 470 m. Complex **3**: Yield: 24%. Anal. Calcd. for $C_{45}H_{37}Eu_{0.0196}Tb_{0.9804}N_4O_8$: C, 58.71%; H, 4.05%; N, 6.09%. Found: C, 58.66%; H, 4.01%; N, 6.02%. FT-IR (KBr pellets, cm^{-1}): 3436 m, 2925 w, 2350 w, 1650 m, 1581 s, 1531 m, 1384 s, 1182 w, 1105 w, 1014 w, 860 m, 788 s, 730 w, 673 m, 470 m. Complex **4**: yield: 21%. Anal. Calcd. for $C_{45}H_{37}Eu_{0.0009}Tb_{0.9901}N_4O_8$: C, 58.79%; H, 4.06%; N, 6.09%. Found: C, 58.71%; H, 4.13%; N, 6.15%. FT-IR (KBr pellets, cm^{-1}): 3471 m, 3060 w, 2925 w, 1650 m, 1581 m, 1527 m, 1425 s, 1182 w, 1014 w, 860 m, 813 w, 786 s, 730 m, 671 m, 468 m. Complex **5**: yield: 25%. Anal. Calcd. for $C_{45}H_{37}TbN_4O_8$: C, 58.70%; H, 4.05%; N, 6.09%. Found: C, 58.66%; H, 4.11%; N, 6.17%. FT-IR (KBr pellets, cm^{-1}): 3430 m, 3060 w, 2925 w, 1650 m, 1581 m, 1529 m, 1421 s, 1182 w, 1105 w, 1014 w, 850 m, 706 s, 730 m, 671 m, 468 m.

2. 3 X-ray crystallography

X-ray single-crystal diffraction data for **1** were collected on a Rigaku SCX-mini diffractometer at 293(2) K with Mo-*Kα* radiation (λ = 0.71073 Å) by an ω scan mode. The crystal data were solved by direct methods and refined by full-matrix least-squares technique on F^2 using the SHELXS and SHELXL. More details on the crystallographic studies as well as atomic displacement parameters are given in the CIF file. All carbon-bonded hydrogen atoms were added theoretically, riding on the concerning atoms and refined with

fixed thermal factors. Crystal data for **1**: triclinic system, $P\bar{1}$ space group with a = 9.0694(6), b = 14.7630(9), c = 15.9047(7) Å, α = 69.049(5)°, β = 81.891(5)°, γ = 83.602(5)°, V = 1964.5(2) Å^3, Z = 2, $C_{45}H_{37}EuN_4O_8$, M_r = 913.75, D_c = 1.545 g/cm^3, F(000) = 924, $GOOF$ = 0.93. Selected bond lengths and bond angles of **1** are given in Table 1.

Table 1. Selected Bond Lengths (Å) and Bond Angles (°) for 1

Bond	Dist.	Bond	Dist.	Bond	Dist.
Eu(1)–O(4)^{i}	2.410(7)	Eu(1)–O(3)^{i}	2.593(8)	Eu(1)–O(5)^{ii}	2.501(8)
Eu(1)–O(6)^{ii}	2.428(7)	Eu(1)–O(1)	2.462(7)	Eu(1)–N(1)	2.591(9)
Eu(1)–O(7)	2.467(8)	Eu(1)–O(2)	2.494(7)	Eu(1)–N(2)	2.583(9)
Angle	(°)	Angle	(°)	Angle	(°)
O(4)^{i}–Eu(1)–O(6)^{ii}	123.2(2)	O(6)^{ii}–Eu(1)–O(1)	136.2(3)	O(1)–Eu(1)–N(1)	86.7(3)
O(6)^{ii}–Eu(1)–O(7)	71.2(3)	O(4)^{i}–Eu(1)–O(2)	121.3(3)	O(2)–Eu(1)–N(1)	83.4(3)
O(1)–Eu(1)–O(2)	52.2(3)	O(4)^{i}–Eu(1)–O(5)^{ii}	125.2(3)	N(2)–Eu(1)–N(1)	63.8(3)
O(1)–Eu(1)–O(5)^{ii}	83.2(3)	O(6)^{ii}–Eu(1)–O(3)^{i}	73.0(3)	O(7)–Eu(1)–O(3)^{i}	135.9(3)
O(4)^{i}–Eu(1)–O(1)	75.0(2)	O(2)–Eu(1)–O(5)^{ii}	76.5(3)	O(5)^{ii}–Eu(1)–O(3)^{i}	85.4(3)
O(4)^{i}–Eu(1)–O(7)	140.7(3)	O(6)^{ii}–Eu(1)–N(2)	76.8(2)	N(1)–Eu(1)–O(3)^{i}	114.0(2)
O(1)–Eu(1)–O(7)	122.3(3)	O(7)–Eu(1)–N(2)	69.8(3)	O(2)–Eu(1)–N(2)	133.0(3)
O(6)^{ii}–Eu(1)–O(2)	113.1(3)	O(5)^{ii}–Eu(1)–N(2)	130.1(2)	O(4)^{i}–Eu(1)–N(1)	68.3(3)
O(7)–Eu(1)–O(2)	70.9(3)	O(6)^{ii}–Eu(1)–N(1)	136.0(3)	O(2)–Eu(1)–O(3)^{i}	149.1(3)
O(6)^{ii}–Eu(1)–O(5)^{ii}	53.3(2)	O(7)–Eu(1)–N(1)	77.3(3)	N(2)–Eu(1)–O(3)^{i}	77.7(3)
O(7)–Eu(1)–O(5)^{ii}	93.3(3)	O(5)^{ii}–Eu(1)–N(1)	159.7(3)	O(1)–Eu(1)–N(2)	145.9(3)
O(4)^{i}–Eu(1)–N(2)	78.2(3)	O(4)^{i}–Eu(1)–O(3)^{i}	52.1(2)	O(1)–Eu(1)–O(3)^{i}	101.4(3)

Symmetry codes: (i) x, y – 1, z + 1; (ii) x + 1, y – 1, z

3 RESULTS AND DISCUSSION

3. 1 Description of the crystal structure

Single-crystal X-ray diffraction analysis reveals that **1** crystallizes in the triclinic system with space group $P\bar{1}$. In the asymmetric unit, there are one Eu^{3+} ion, one BTB^{3-} ligand, one 1,10-phenanthroline (phen) and one coordinated DMF as well as a free DMF. The central Eu^{3+} ion exhibits a nine-coordinate environment forming a twisted triangular prism with six oxygen atoms from three BTB^{3-}, two nitrogen atoms from a phen and an oxygen atom from a coordinated DMF (Fig. 1a). Each BTB^{3-} connects three Eu^{3+} ions through chelating coordination of carboxylic acids (Fig. 1b). As shown in Fig. 1c, Eu^{3+} cations are connected as a node through three BTB^{3-} to form a 2*D* plane structure. Each 2*D* stratified structure is stacked into a 3*D* supramolecular structure through π-π interactions with the shortest centroid-to-centroid distance of 3.646 Å (Fig. 1d). Topologically, Eu^{3+} and BTB^{3-} can be simplified as 3-connected nodes, and the 2*D* plane as a *hcb* net (Fig. 1e).

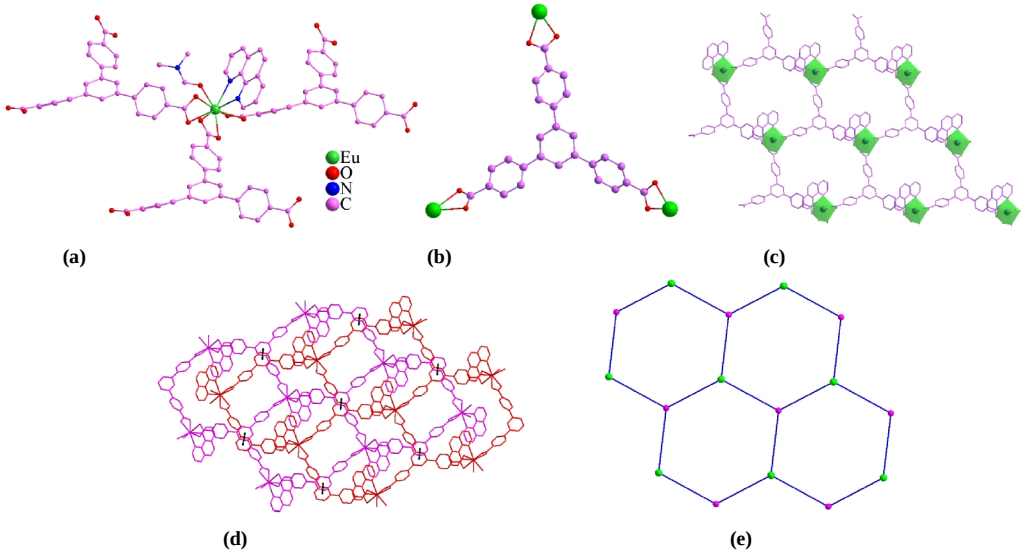

Fig. 1. (a) Coordinated environments of Eu^{3+}; (b) Coordinated environments of BTB^{3-}; (c) 2*D* framework of 1; (d) 3*D* supramolecular structure through π-π interactions (black dashed lines for π-π interactions); (e) *hcb* net of 2*D* plane

3. 2 PXRD and thermogravimetric analysis

The purity of the bulky crystalline samples of **1** was confirmed by PXRD at room temperature. As shown in Fig. 2, the PXRD pattern of the as-synthesized **1** corresponds well with the simulated one based on the single-crystal diffraction data, which confirms the good purity of **1**.

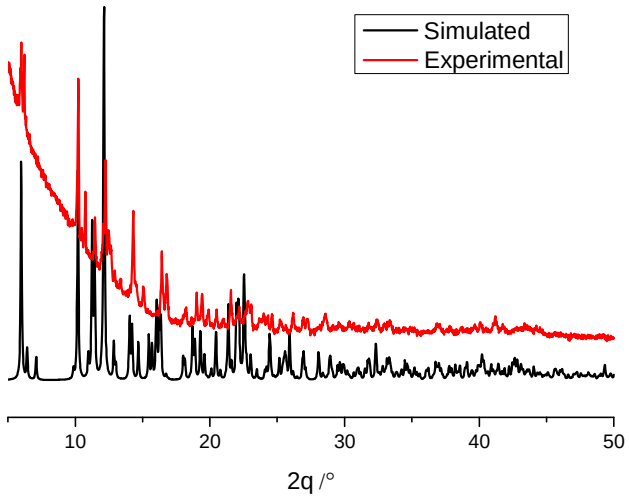

Fig. 2. PXRD patterns of 1

The thermal stability of the complex was evaluated by TG experiment and the results shown in Fig. 3 suggest that the first weight loss of about 16.5% (calculated 16.0%) occurred from room temperature to 500 ℃, corresponding to the removal of DMF molecules. Subsequently, there is a quick mass loss at 500～700 ℃, which may correspond to the decomposition of the framework.

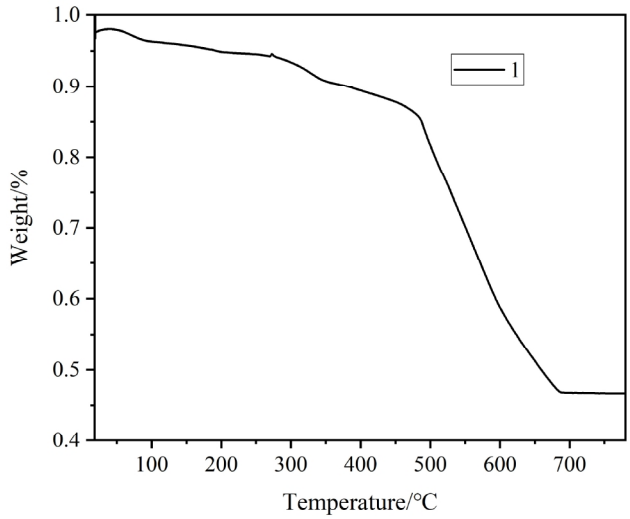

Fig. 3. TGA curve of 1

3. 3 Fluorescence properties

3. 3. 1 Solid-state photoluminescent spectra

The luminescent spectra of **1** were determined in the solid state at room temperature and the results are shown in Fig. 4. When excited at 300 nm, the emission peaks at 579, 588, 594, 615, 618, 650, 683 and 692 nm correspond to the transition from $^5D_0 \rightarrow {}^7F_J$ (J = 0～4) of Eu^{3+} ions. The most intense emissions in the luminescent spectra around 615 and 618 nm are ascribed to the electric dipolar $^5D_0 \rightarrow {}^7F_2$ transition, which is responsible for the red emission observed for these MOFs[44]. The splitting emission band for the $^5D_0 \rightarrow {}^7F_1$, $^5D_0 \rightarrow {}^7F_2$ and $^5D_0 \rightarrow {}^7F_4$ transition indicates only one type of coordination environment for the Eu^{3+} cation in **1**[44]. The results are in good agreement with the single-crystal X-ray analyses.

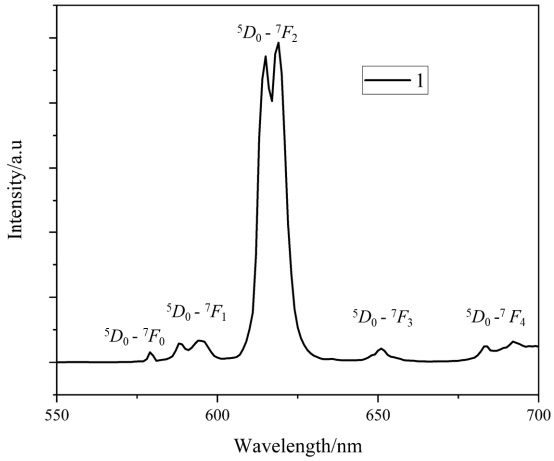

Fig. 4. Solid-state emission spectra of 1

3. 3. 2 Fluorescence sensing properties of 1

The fluorescence properties of **1** in different metal ion solutions were also investigated. The corresponding MOF/M^{m+} was prepared by introducing **1** (3 mg) powder into 3 mL ethanol solution of MNO_x (M^{m+} = K^+, Cd^{2+}, Mg^{2+}, Mn^{2+}, Ni^{2+}, Ca^{2+}, Zn^{2+}, Cu^{2+}, Fe^{3+}) with each concentration to be 1 mmol/L, which was uniformly dispersed under ultrasonication for 5 min. A series of luminescent responses were recorded and compiled in Fig. 5a, which suggests that at 615 nm, **1** exhibited luminescence intensities for different metal ions with great degree of variation in their bursting effect. Interestingly, Fig. 5b shows that **1** exhibits a drastic quenching effect in the Fe^{3+} ion solution, which can be of great help in practical application for the sensing of Fe^{3+}, which was further evaluated in the subsequent experiments. Due to the coexistence of multiple metal ions in real solution system, competing experiments were conducted with respectively adding various metal ions to the suspension of **1**, followed by the treatment of equivalent amount of Fe^{3+}. As can be seen from Fig. 5c, the presence of other metal ions has almost no significant effect on the selectivity of **1** to Fe^{3+}, further indicating the high fluorescence selectivity of **1** to Fe^{3+}.

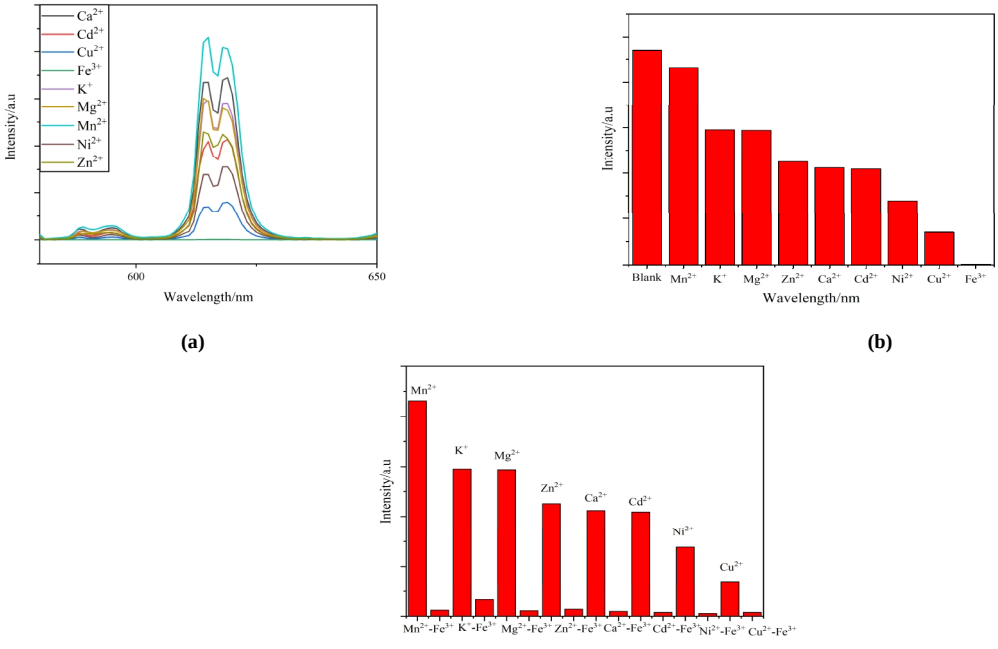

Fig. 5. (a) Luminescence spectra of 1 dispersed in ethanol solutions of different metal ions; (b) Maximum emission intensity of 1 in multiple metal cation-ethanol solution; (c) Luminescence intensity (615 nm) of 1 dispersed in EtOH with the addition of different ions (Mg^{2+}, Cd^{2+}, Zn^{2+}, Mn^{2+}, K^+, Ni^{2+}, Ca^{2+}, Cu^{2+}) (1 mmol/L) and Fe^{3+} incorporated systems (1 mmol/L)

To better understand the sensing sensitivities of **1** for Fe^{3+} ions, a series of titrating experiments were carried out in ethanol solutions with variable concentrations of Fe^{3+} ions. **1** (3 mg) was sonicated in EtOH (3 mL) followed by the addition of different volumes of Fe^{3+} (1 mmol/L) and the emission spectra were measured as displayed in Fig. 6. It is noted that the fluorescence intensity of **1** is completely quenched at Fe^{3+} ion concentration of 0.1 mM (300 μL). The relationship between the quenching effect and Fe^{3+} concentration was further investigated through the Stern-Volmer equation *i.e.* $I_0/I = 1 + K_{SV}$ [M], where I_0 and I represent the initial luminescence intensity and luminescence intensity after adding analyte, respectively, [M] is the concentration of analyte, and K_{SV} stands for the Stern-Volmer constant[45]. The Stern-Volmer plot of **1** in Fig. 7 shows that at higher Fe^{3+} ion concentration, there is a nonlinear upward curvature, indicating that the mechanism of luminescence quenching may be a combination of dynamic quenching and static quenching[32]. The K_{SV} value was found to be 3.91×10^4 M^{-1} for **1** at low concentrations of Fe^{3+} ions. The value is comparable with those reported for MOF-based sensor materials in the literatures (Table 2)[46-49]. The limits of detection (*LOD*) can be determined by $LOD = 3\sigma/k$ (k is the slope of the linear curve and σ is the standard deviation of the blank sample)[50]. With the slope of the fitting line and the measurement error of the intensity with blank samples, the detection limit for Fe^{3+} was calculated to be 1.7 μM. On the other hand, the quenching efficiency of **1** can be maintained above 80% through five cycles of experiments (Fig. 8).

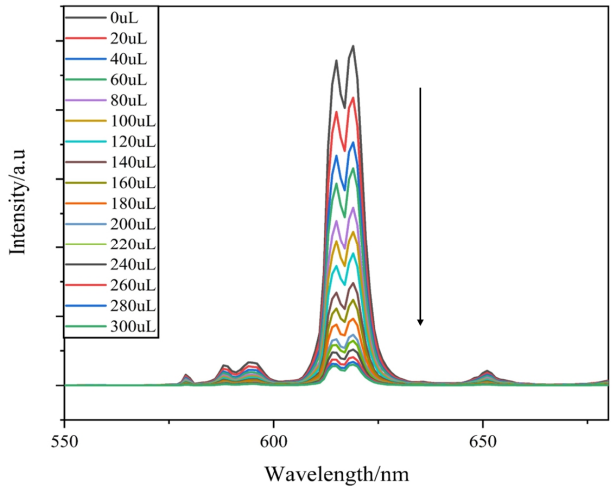

Fig. 6. Emission spectra of 1 dispersed in EtOH upon increasing addition of Fe^{3+}

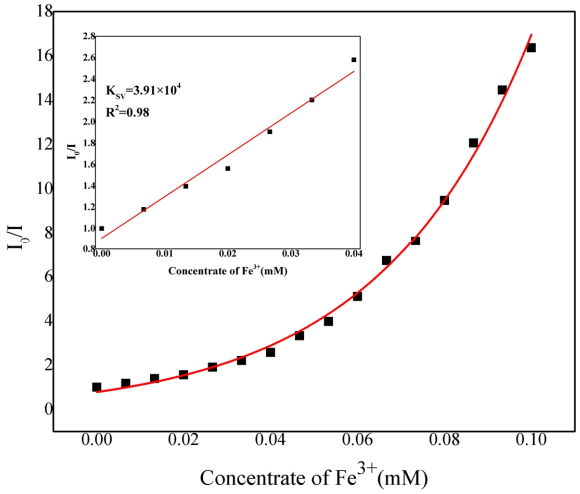

Fig. 7. Stern-Volmer plots of 1; the inset demonstrates the quenching linearity relationship at low concentration of Fe^{3+} ion

Table 2. K_{SV} Values for Fe^{3+} in Comparison with Literatures

Complex	K_{SV} (M^{-1})	Ref.
$\{Ni(1,4\text{-bib})_{1.5}(TPA\text{-}Cl_2)\cdot H_2O\}_n$	7×10^4	[46]
JLU-MOF71	5.77×10^4	[47]
$[Zn_4(bptc)_2(NMP)_3(DMF)(H_2O)_2]_n$	4.12×10^3	[48]
$[Cd_8(bptc)_4(NMP)_6(DMF)_4(H_2O)_2]_n$	6.57×10^3	[48]
$\{[Zn_2(bptc)(DMA)(H_2O)_2]\cdot(DMA)_2\cdot H_2O\}_n$	3.76×10^3	[48]
$\{[CoL_2Cl_2]ž4CH_3OH\}_\infty$	1.07×10^4	[49]
$\{[NiL_2Cl_2]ž4CH_3OH\}_\infty$	1.67×10^4	[49]
$\{[CoL_2Br_2]ž4CH_3OH\}_\infty$	3.33×10^4	[49]
Eu-MOF	3.91×10^4	This work

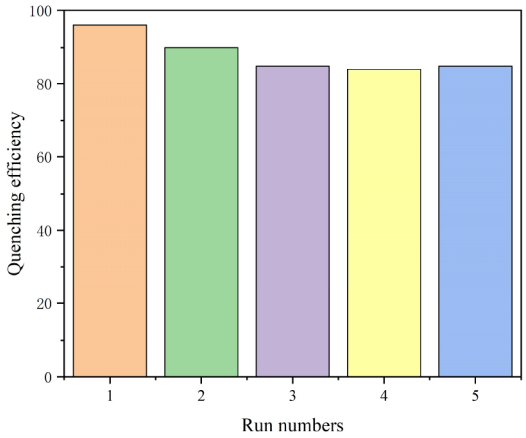

Fig. 8. Quenching efficiency of 1 dispersed in EtOH with the addition of 0.1 mM Fe^{3+} for 5 runs

3. 4 Color tuning

Because of the similar coordination environment and coordination number of the Ln^{3+} ions, different Ln ions can be combined in the same MOF. Using an analogous synthetic protocol to that used for the preparation of **1**, various ratios of Eu^{3+} and Tb^{3+} were introduced to the solutions of H_3BTB in DMF: water and various complexes of Eu_xTb_{1-x} were synthesized (complexes **2**～**5**). After isolation of the crystalline products, PXRD were performed to analyze the structural analogy of these complexes to homometallic **1** (Fig. 9). The solid samples were then studied by fluorescence spectroscopy and the effect of altering the lanthanide ion ratios in Eu_xTb_{1-x} was manifested in the variation of the emission spectra (Fig. 10). It was noted that as the molar ratio of Eu^{3+} increased from 0.0009 to 0.0909, the relative emission intensity of the strongest emission of Tb^{3+} at 544 nm gradually weakened, while that of the Eu^{3+} ion at 615 nm gradually enhanced. The general shift in color can be safely assumed giving the trend of the spectra, and chromaticity coordinates were calculated and plotted in the CIE coordinate diagram to more clearly present the colors of emission (Fig. 11).

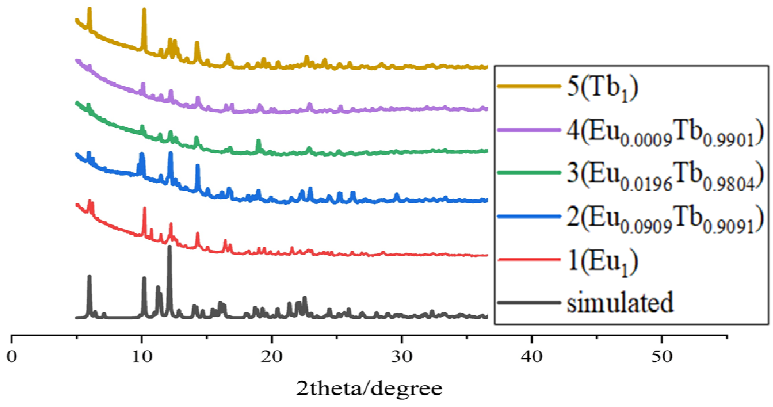

Fig. 9. PXRD pattern of complexes 1～5

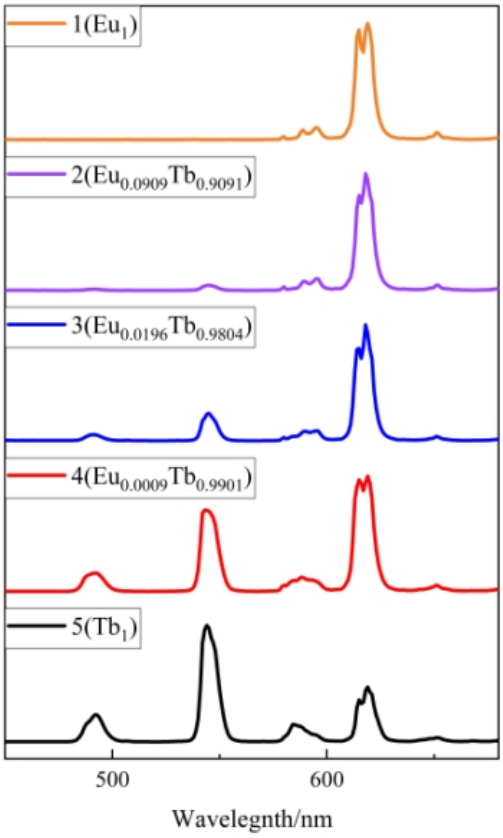

Fig. 10. Emission spectra of complexes 1～5

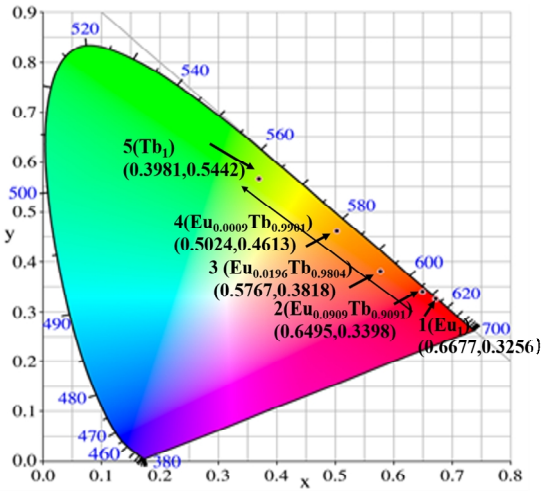

Fig. 11. CIE chromaticity coordinates of complexes 1～5 displaying a green shift in the color of emission

4 CONCLUSION

In summary, a novel 2*D* Eu-MOF (**1**) was successfully synthesized under solvothermal conditions using H_3BTB as the ligand. X-ray single-crystal analysis demonstrated that **1** is a 3*D* supramolecular network formed by the stacking of 2*D* layers through π-π interactions. The luminescence explorations revealed that **1** possesses high selectivity and sensitivity for the sensing of Fe^{3+} by quenching mechanism with $K_{SV} = 3.91 \times 10^4\ M^{-1}$. Furthermore, a series of co-doped Ln-MOFs with tunable luminescence were also fabricated and tested, which showed that their luminescent color can be effectively tuned from red to green by controlling the ratios of Eu^{3+}:Tb^{3+}. This study provides important guidelines for the fabrication of Eu-MOF for the highly efficient sensing of Fe^{3+} in practical applications.

REFERENCES

(1) Cheng, X. F.; Hu, J. S.; Li, J. X.; Zhang, M. D. Tunable emission and selective luminescence sensing for nitro-pollutants and metal ions based on bifunctional lanthanide metal-organic frameworks. *J. Lumin.* **2020**, 221, 117100- 10.

(2) Yao, S. L.; Xiong, Y. C.; Tian, X. M.; Liu, S. J.; Xu, H.; Zheng, T. F.; Chen, J. L.; Wen, H. R. A multifunctional benzothiadiazole-based fluorescence sensor for Al^{3+}, Cr^{3+} and Fe^{3+}. *CrystEngComm* **2021**, 23, 1898- 1905.

(3) Yao, Q. X.; Tian, M. M.; Wang, Y.; Meng, Y. J.; Wang, J.; Yao, Q. Y.; Zhou, X.; Yang, H.; Wang, H. W.; Li, Y. W.; Zhang, J. A robust, water-stable, and multifunctional praseodymium-organic framework showing permanent porosity, CO_2 adsorption properties, and selective sensing of Fe^{3+} ion. *Chin. J. Struct. Chem.* **2020**, 39, 1862- 1870.

(4) Chandra Rao, P.; Mandal, S. Europium-based metal-organic framework as a dual luminescence sensor for the selective detection of the phosphate anion and Fe^{3+} ion in aqueous media. *Inorg. Chem.* **2018**, 57, 11855- 11858.

(5) Zhang, Z.; Fang, Q. H.; Zhuang, Z. Y.; Han, Y.; Li, L. Y.; Yu, Y. Europium activated aluminum organic frameworks for highly selective and sensitive setection of Fe^{3+} and Cr(VI) in aqueous solution. *Chin. J. Struct. Chem.* **2020**, 39, 1958- 1964.

(6) Guo, X. H.; Li, Y. S.; Peng, Q. Y.; Duan, Z. M.; Li, M. X.; Shao, M.; He, X. Dual functional three-dimensional LnMOFs for luminescence sensing of nitrobenzene and Fe^{3+} ions. *Polyhedron* **2017**, 133, 238- 244.

(7) Wu, N.; Guo, H.; Wang, X. Q.; Sun, L.; Zhang, T. T.; Peng, L. P.; Yang, W. A water-stable lanthanide-MOF as a highly sensitive and selective luminescence sensor for detection of Fe^{3+} and benzaldehyde. *Colloids Surf. A: Physicochem. Eng. Asp.* **2021**, 616, 126093- 7.

(8) Guan, B. B.; Li, Q.; Xu, Y. T.; Chen, L. H.; Wu, Z. S.; Fan, Z. L.; Zhu, W. Highly selective and sensitive detection towards cationic Cu^{2+} and Fe^{3+} contaminants via an In-MOF based dual-responsive fluorescence probe. *Inorg. Chem. Commun.* **2020**, 122, 108273- 7.

(9) Xia, Z. Q.; Ren, C. T.; Xu, W. F.; Li, F.; Qiao, C. F.; Wei, Q.; Zhou, C. S.; Chen, S. P.; Gao, S. L. Ultrasensitive Fe^{3+} luminescence sensing and supercapacitor performances of a triphenylamine-based Tb^{III}-MOF. *J. Solid State Chem.* **2020**, 282, 121083- 7.

(10) Yin, X. J.; Li, S. X.; Liao, B. L. Water-stable Ln-exclusive metal-organic framework for highly selective sensing of Fe^{3+} ions. *Dyes Pigm.* **2020**, 174, 108035- 7.

(11) Yu, M. H.; Liu, X. T.; Space, B.; Chang, Z.; Bu, X. H. Metal-organic materials with triazine-based ligands: from structures to properties and applications. *Coord. Chem. Rev.* **2021**, 427, 213518- 45.

(12) Wang, C. C.; Wang, X.; Liu, W. The synthesis strategies and photocatalytic performances of TiO_2/MOFs composites: a state-of-the-art review. *Chem. Eng. J.* **2020**, 391, 1385- 8947.

(13) Kong, L. J.; Liu, M.; Huang, H.; Xu, Y. H.; Bu, X. H. Metal/covalent-organic framework based cathodes for metal-ion batteries. *Adv. Energy Mater.* **2021**, 2100172- 26.

(14) Xiao, Q. Q.; Dong, G. Y.; Li, Y. H.; Cui, G. H. Cobalt(II)-based 3*D* coordination polymer with unusual 4,4,4-connected topology as a dual-responsive fluorescent chemosensor for acetylacetone and $Cr_2O_7^{2-}$. *Inorg. Chem.* **2019**, 58, 15696- 15699.

(15) Zhu, H.; Li, Y. H.; Xiao, Q. Q.; Cui, G. H. Three luminescent Cd(II) coordination polymers containing aromatic dicarboxylate and flexible bis(benzimidazole) ligands as highly sensitive and selective sensors for detection of $Cr_2O_7^{2-}$ oxoanions in water. *Polyhedron* **2020**, 187, 114648- 8.

(16) Liu, A. J.; Xu, F.; Han, S. D.; Pan, J.; Wang, G. M. Mixed-ligand strategy for the construction of photochromic metal-organic frameworks driven by electron-transfer between nonphotoactive units. *Cryst. Growth Des.* **2020**, 20, 7350- 7355.

(17) Chen, D. D.; Yi, X. H.; Wang, C. C. Preparation of metal-organic frameworks and their composites using mechanochemical methods. *Chin. J. Inorg. Chem.* **2020**, 36, 1805- 1821.

(18) Ju, P.; Liu, X. C.; Zhang, E. S. A novel 3*D* Zn-based luminescence metal-organic framework: synthesis, structure and fluorescence enhanced sensing of ammonia vapor in air. *Chin. J. Struct. Chem.* **2020**, 39, 1458- 1464.

(19) Rocha, J.; Carlos, L. D.; Paz, F. A.; Ananias, D. Luminescent multifunctional lanthanides-based metal-organic frameworks. *Chem. Soc. Rev.* **2011**, 40, 926- 940.

(20) Zhai, L. J.; Jiao, C. X.; Liang, T. F.; Zhang, J.; Niu, X. Y.; Hu, T. P.; Niu, Y. L. Two new coordination polymers based on H_4BIPA-TC: syntheses and fluorescence sensing for nitroaromatic compounds and Fe^{3+} ion. *Chin. J. Struct. Chem.* **2020**, 39, 772- 782.

(21) Lv, X. L.; Feng, L.; Wang, K. Y.; Xie, L. H.; He, T.; Wu, W.; Li, J. R.; Zhou, H. C. A series of mesoporous rare-earth metal-organic frameworks constructed from organic secondary building units. *Angew. Chem. Int. Ed.* **2021**, 60, 2053- 2057.

(22) Lv, X. L.; Feng, L.; Xie, L. H.; He, T.; Wu, W.; Wang, K. Y.; Si, G. R.; Wang, B.; Li, J. R.; Zhou, H. C. Linker desymmetrization: access to a series of rare-earth tetracarboxylate frameworks with eight-connected hexanuclear nodes. *J. Am. Chem. Soc.* **2021**, 143, 2784- 2791.

(23) Kumar, M.; Li, L. Q.; Zareba, J. K.; Tashi, L.; Sahoo, S. C.; Nyk, M.; Liu, S. J.; Sheikh, H. N. Lanthanide contraction in cction: structural variations in 13 lanthanide(III) thiophene-2,5-dicarboxylate coordination polymers (Ln = La-Lu, except Pm and Tm) featuring magnetocaloric effect, slow magnetic relaxation, and luminescence-lifetime-based thermometry. *Cryst. Growth Des.* **2020**, 20, 6430- 6452.

(24) Li, Y. P.; Yang, H. R.; Zhao, Q.; Song, W. C.; Han, J.; Bu, X. H. Ratiometric and selective fluorescent sensor for Zn^{2+} as an "off-on-off" switch and logic gate. *Inorg. Chem.* **2012**, 51, 9642- 9648.

(25) D'Vries, R. F.; Gomez, G. E.; Mondragon, L. P.; Onna, D.; Barja, B. C.; Soler-Illia, G. J. A. A.; Ellena, J. 1*D* lanthanide coordination polymers based on lanthanides and 4′-hydroxi-4-biphenylcarboxylic acid: synthesis, structures and luminescence properties. *J. Solid State Chem.* **2019**, 274, 322- 328.

(26) Yang, Y.; Wang, Y.; Feng, Y.; Song, X.; Cao, C.; Zhang, G.; Liu, W. Three isostructural Eu^{3+}/Tb^{3+} co-doped MOFs for wide-range ratiometric temperature sensing. *Talanta* **2020**, 208, 120354- 6.

(27) Zhou, X. J.; Chen, L. N.; Feng, Z. S.; Jiang, S.; Lin, J. Z.; Pang, Y.; Li, L.; Xiang, G. T. Color tunable emission and low-temperature luminescent sensing of europium and terbium carboxylic acid complexes. *Inorg. Chim. Acta* **2018**, 469, 576- 582.

(28) Zhu, Y. Y.; Xia, T. F.; Zhang, Q.; Cui, Y. J.; Yang, Y.; Qian, G. D. A Eu/Tb mixed lanthanide coordination polymer with rare 2*D* thick layers: synthesis, characterization and ratiometric temperature sensing. *J. Solid State Chem.* **2018**, 259, 98- 103.

(29) Pang, X. L.; Yu, T.; Shen, F. J.; Yu, X. D.; Li, Y. J. Fluorescence sensing of fluoride ions and N,N-dimethylformamide by novel luminescent lanthanide(III) xerogels. *J. Lumin.* **2018**, 204, 169- 175.

(30) Zhai, B.; Xu, H.; Li, Z. Y.; Cao, C. S.; Zhao, B. A water-stable metal-organic framework: serving as a chemical sensor of PO_4^{3-} and a catalyst for CO_2 conversion. *Sci. China. Chem.* **2017**, 60, 1328- 1333.

(31) Chen, D. M.; Zheng, Y. P.; Fang, S. M. A polyhedron-based porous Tb(III)-organic framework with dual emissions for highly selective detection of Al^{3+} ion. *Inorg. Chem. Commun.* **2020**, 117, 107967- 21.

(32) Guo, H.; Wu, N.; Xue, R.; Liu, H.; Li, L.; Wang, M. Y.; Yao, W. Q.; Li, Q.; Yang, W. Multifunctional Ln-MOF luminescent probe displaying superior capabilities for highly selective sensing of Fe^{3+} and Al^{3+} ions and nitrotoluene. *Colloids Surf. A: Physicochem. Eng. Asp.* **2020**, 585, 124094- 8.

(33) Liang, G. M.; Wang, S.; Xu, M. Y.; Chen, H. L.; Liang, G. Y.; Gui, L. C.; Wang, X. J. 2*D* lanthanide coordination polymers constructed from a semi-rigid tricarboxylic acid ligand: crystal structure, luminescence sensing and color tuning. *CrystEngComm* **2020**, 22, 6161- 6169.

(34) Chen, D. M.; Sun, C. X.; Peng, Y.; Zhang, N. N.; Si, H. H.; Liu, C. S.; Du, M. Ratiometric fluorescence sensing and colorimetric decoding methanol by a bimetallic lanthanide-organic framework. *Sensor Actuat. B-Chem.* **2018**, 265, 104- 109.

(35) Zhan, C.; Ou, S.; Zou, C.; Zhao, M.; Wu, C. D. A luminescent mixed-lanthanide-organic framework sensor for decoding different volatile organic molecules. *Anal. Chem.* **2014**, 86, 6648- 6653.

(36) Zhou, J.; Li, H.; Zhang, H.; Li, H.; Shi, W.; Cheng, P. A bimetallic lanthanide metal-organic material as a self-calibrating color-gradient luminescent sensor. *Adv. Mater.* **2015**, 27, 7072- 7077.

(37) Zhang, F. X.; Li, J. Y.; Zhao, Z. R.; Wang, F. Q.; Pu, Y. Y.; Cheng, H. L. Mixed-LnMOFs with tunable color and white light emission together with multi-functional fluorescence detection. *J. Solid State Chem.* **2019**, 280, 120972- 5.

(38) Yang, Q. Y.; Pan, M.; Wei, S. C.; Li, K.; Du, B. B.; Su, C. Y. Linear dependence of photoluminescence in mixed Ln-MOFs for color tunability and barcode application. *Inorg. Chem.* **2015**, 54, 5707- 5716.

(39) Zhao, S.; Hao, X. M.; Liu, J. L.; Wu, L. W.; Wang, H.; Wu, Y. B.; Yang, D.; Guo, W. L. Construction of Eu(III)- and Tb(III)-MOFs with photoluminescence for sensing small molecules based on furan-2,5-dicarboxylic acid. *J. Solid State Chem.* **2017**, 255, 76- 81.

(40) Dzesse T, C. N.; Nfor, E. N.; Bourne, S. A. Tripodal carboxylate MOFs with Co(II): transmetallation and gas sorption studies. *Polyhedron* **2020**, 189, 114724- 8.

(41) Wu, Y. P.; Tian, J. W.; Liu, S.; Li, B.; Zhao, J.; Ma, L. F.; Li, D. S.; Lan, Y. Q.; Bu, X. Bi-microporous metal-organic frameworks with cubane $[M_4(OH)_4]$ (M = Ni, Co) clusters and pore-space partition for electrocatalytic methanol oxidation reaction. *Angew. Chem. Int. Ed.* **2019**, 58, 12185- 12189.

(42) Guo, X. Y.; Zhao, F.; Liu, H. T.; Wang, Y. Q.; Liu, Z. L.; Gao, E. Q. Five new 2*D* and 3*D* coordination polymers based on two new multifunctional pyridyl-tricarboxylate ligands: hydrothermal syntheses, structural diversity, luminescent and magnetic properties. *RSC Adv.* **2017**, 7, 19039- 19049.

(43) He, K. H.; Li, Y. W.; Chen, Y. Q.; Song, W. C.; Bu, X. H. Employing zinc clusters as SBUs to construct (3,8) and (3,14)-connected coordination networks: structures, topologies, and luminescence. *Cryst. Growth Des.* **2012**, 12, 2730- 2735

(44) Zhang, J.; Zheng, B.; Zhao, T. T.; Li, G. H.; Huo, Q. S.; Liu, Y. L. Topological diversities and luminescent properties of lanthanide metal-organic frameworks based on a tetracarboxylate ligand. *Cryst. Growth Des.* **2014**, 14, 2394- 2400.

(45) Hou, L. L.; Song, Y. H.; Lang, F. X.; Wang, Z. R.; Wang, L. Fluorometric determination of Fe^{3+} and polychlorinated benzenes based on Tb^{3+}-pyromellitic acid coordination polymer. *J. Ind. Eng. Chem.* **2020**, 90, 145- 151.

(46) Cui, J. W.; Hou, S. X.; Li, Y. H.; Cui, G. H. A multifunctional Ni(II) coordination polymer: synthesis, crystal structure and applications as a luminescent sensor, electrochemical probe, and photocatalyst. *Dalton Trans.* **2017**, 46, 16911- 16924.

(47) Yu, C.; Sun, X.; Zou, L.; Li, G.; Zhang, L.; Liu, Y. A pillar-layered Zn-LMOF with uncoordinated carboxylic acid sites: high performance for luminescence sensing Fe^{3+} and TNP. *Inorg. Chem.* **2019**, 58, 4026- 4032.

(48) Huang, W. H.; Ren, J.; Yang, Y. H.; Li, X. M.; Wang, Q.; Jiang, N.; Yu, J. Q.; Wang, F.; Zhang, J. Water-stable metal-organic frameworks with selective sensing on Fe^{3+} and nitroaromatic explosives, and stimuli-responsive luminescence on lanthanide encapsulation. *Inorg. Chem.* **2019**, 58, 1481- 1491.

(49) Nandi, S.; Reinsch, H.; Banesh, S.; Stock, N.; Trivedi, V.; Biswas, S. Rapid and highly sensitive detection of extracellular and intracellular H_2S by an azide-functionalized Al(III)-based metal-organic framework. *Dalton Trans.* **2017**, 46, 12856- 12864.

(50) He, T. S.; Lan, Y. L.; Li, Z. Y.; Zhu, L. N.; Li, X. Z. Chiral coordination polymers from a new 2-deoxy-d-ribose derivative linker: syntheses, structures, and Fe^{3+} fluorescent probe functions. *Cryst. Growth Des.* **2021**, 21, 2233- 2242.